Engineered Science
DOI: https://dx.doi.org/10.30919/es8d821

Trapdoor Stability of Drained Cohesive-Frictional Soils Using Terzaghi's Superposition Method

Jim Shiau,[1] Rungkhun Banyong,[2] Suraparb Keawsawasvong[2,*] and Viroon Kamchoom[3]

Abstract

Most previous trapdoor stability studies were centered on undrained clay in two dimensions in the past few decades. Very few works were reported for cohesive-frictional soils in two- and three-dimensions. This paper sets out to examine the stability of trapdoors in c-ϕ soils under both 2D planar and 3D circular (axisymmetric) conditions using a superposition method that is similar to Terzaghi's bearing capacity coefficients approach. Using lower bound and upper bound limit analysis with finite elements, the proposed three coefficients (F_c, F_s, and F_γ) are determined with respect to a series of parametric changes of depth ratios and soil internal friction angles. Novel design charts and tables are presented, and several examples are provided to show how to use the three coefficients to evaluate soil stability under planar and circular trapdoors. The numerical results presented in the paper should be of interest to the geotechnical engineering community.

Keywords: Active; Trapdoor; Stability coefficients; Limit analysis; Axisymmetry.
Received: 28 December 2022; Revised: 09 February 2023; Accepted: 17 February 2023.
Article type: Research article.

1. Introduction

The stability of underground openings has been a major focus in the geotechnical engineering research community. It is closely related to both the safety of existing infrastructures and the effective execution of an underground project. The problem of an opening trapdoor in active failure can represent several geotechnical engineering examples such as the gravity flow of granular material via hoppers,[1] the roof stability of underground mining works,[2-3] and the undrained sinkhole stability problems.[4-8] Several researchers have studied the problem of active trapdoors using physical model testing[9-12] and numerical or analytical methods.[13-26]

The use of three stability coefficients with the principle of superposition for geotechnical stability analysis and design is not new, and it was applied to several tunneling problems in drained conditions.[27-29] The process of analysis is similar to Terzaghi's bearing capacity problem, in which the footing capacity of a strip footing consists of three components: namely the cohesion, the surcharge, and the soil unit weight.

This approach has not yet been applied to the classical active trapdoor problems. The active stability equation adopted for determining the minimum support pressure (σ_t) of underground tunneling is presented in Eq. (1).[27-28]

$$\sigma_t = -cF_c + \sigma_s F_s + \gamma D F_\gamma \quad (1)$$

where c is the soil cohesion; F_c is the cohesion coefficient; σ_s is the surcharge; F_s is the surcharge coefficient; γ is the unit weight of soil; D is the tunnel diameter; F_γ is the soil unit weight coefficient. Note that the negative sign for cohesion in equation (1) is presented because of the active failure nature where the cohesion strength acts against the surcharge and the soil unit weight.

The "active" stability coefficient approach of Shiau and Al-Asadi[27,28] is the same as Terzaghi's "passive" bearing capacity approach, except for the presented negative sign in front of cohesion, as stated in equation (1). The solution process involves the determination of the three coefficients, namely the stability coefficients for the cohesion (F_c), the surcharge (F_s), and the soil unit weight (F_γ). To obtain the cohesion coefficient (F_c), it is necessary to "artificially" impose zero σ_s and zero γ in the computation. A similar process applies to the

[1] *School of Engineering, University of Southern Queensland, QLD, Toowoomba, 4350, Australia.*
[2] *Research Unit in Sciences and Innovative Technologies for Civil Engineering Infrastructures, Department of Civil Engineering, Faculty of Engineering, Thammasat School of Engineering, Thammasat University, Pathumthani 12120, Thailand.*
[3] *Excellent Centre for Green and Sustainable Infrastructure, Department of Civil Engineering, School of Engineering, King Mongkut's Institute of Technology Ladkrabang (KMITL), Bangkok, Thailand.*
**Email:* ksurapar@engr.tu.ac.th (S. Keawsawasvong)

computation of F_s and F_γ. The principle of superposition in Eq. (1) is well recognized due to its effectiveness in the determination of drained soil bearing capacity. Indeed, Eq. (1) can be used to transform the problem to either undrained clay, or dry sand, or even to study the effect of surcharge. In comparison to the early work of drained analysis in Anagnostou and Kovári,[30] this process has been successfully adopted to solve several geotechnical stability problems by Shiau and Al-Asadi[27,28] using the very recent development of advanced finite element.[31,32] Note that the theory of finite element limit analysis (FELA) is quite different from that of the displacement-based finite element method (FEM), even though both methods are rooted in the concept of a discrete formulation.[33-42] Sloan[31] stated that the stability analysis using the FELA based on the limit analysis theory requires only the conventional strength parameters such as soil cohesion and friction angle. The deformation parameters such as Poisson's ratio and shear modulus are not required in the limit analysis as it is a direct method for perfectly plastic materials.

It is important to know that most studies on trapdoor problems were linked to 2D planar trapdoors in cohesive soils under undrained conditions. Very few studies were reported for drained cohesive-frictional soils. To our best knowledge, currently, no published paper can be found in relation to soil stability coefficients for planar and circular trapdoors in cohesive-frictional soils. In this practical paper, the stability coefficient approach based on the tunneling work presented by Shiau and Al-Asadi[27,28] is revisited for a planar trapdoor and circular trapdoor in an axisymmetric condition. The study aims to develop brand new stability coefficients (F_c, F_s, and F_γ) for accurate assessment of soil stability at collapse under both plane strain and axisymmetric conditions. With the advanced finite element limit analysis and adaptive meshing technique, the produced stability coefficients are confidently provided in tables and figures to assist practicing engineers to evaluate soil stability at the preliminary design stage.

2. 2D Planar trapdoor

2.1 Problem statement and FELA modeling

The limit analysis is most advantageous when both upper bound (UB) and lower bound (LB) solutions can bracket the actual collapse load to within a few percentages. Sloan[43,44] first developed finite elements and linear programming for geotechnical stability analyses. They were extended by Lyamin and Sloan[45,46] and Krabbenhoft *et al.*[47] using nonlinear programming formulation. The underlying bound theorems assume a rigid-perfectly plastic material and have been effectively utilized to study a variety of drained and undrained stability problems in geotechnical engineering.[48-62] Comprehensive documentation of the latest development of the technique can be found in Sloan[31] and OptumCE.[32] A brief description of LB and UB FELA for plane strain problems is given next. the LB analysis, the element in LB is a linear three-node triangular element with nodal stresses including σ_x, σ_y, and τ_{xy}. These nodal stresses are the basic unknown variables for the plane strain problem. To produce the continuity of normal and shear stresses between all elements, the statically admissible stress discontinuities are carried out. Also, the stress equilibrium as well as the Mohr-Coulomb (MC) yield criterion is carried out in LB analysis. The pressure at trapdoors is set to be the objective function, where the yield criterion and the stress equilibrium equations are satisfied. Note that the expression of the MC model is shown in Eq. (2).

$$\sqrt{(\sigma_x-\sigma_y)^2+(\sigma_x-\tau_{xy})^2}-2c\cot\phi-(\sigma_x-\sigma_y)\sin\phi\le 0 \quad (2)$$

In UB analysis, the element in UB is a six-node triangular element. Each node has two basic unknown velocities including the horizontal (u) and vertical velocities (v). At the interfaces of all the elements, velocity discontinuities are kinematically admissible. To capture the MC model in the form of two basic unknown velocities with the assumption of the associated flow rule, Eq. (3) can be carried out as:

$$\Delta v-|\Delta u|\tan\phi=0 \quad (3)$$

Note that Δu and Δv in the above equations are the tangential and normal velocity jumps along the discontinuity. Similar to that in LB analysis, trapdoor pressure is an objective function of UB analysis. To find out more basic equations about UB and LB, readers are referred to Sloan[31] and OptumCE.[32]

Figure 1 presents the problem statement of a 2D planar trapdoor. The idealized planar trapdoor has a cover depth (H) and a width (B). The trapdoor is assumed to be very long so that it can be represented by the plane strain condition. A surcharge (σ_s) is applied vertically to the ground surface, whilst a positive value of (σ_t) represents the normal compressive pressure. The soil mass is represented by the Mohr-Coulomb material with the assumption of the associated flow rule. The material properties are the cohesion c, frictional angle ϕ, and bulk unit weight γ. Also shown in the figure is a potential slip surface of the 2D problem.

A typical FELA mesh and shear dissipation (indication of failure mechanism) used for the planar trapdoor analysis is shown in Fig. 2. The assumption for boundary conditions follows the comment setting used in the FELA or FEM of many geotechnical engineering problems.[48-62] The symmetrical half mesh is used with the following boundary conditions: the far side boundary is fixed in the x-direction, and the boundary at the bottom is fixed in both x- and y-directions. For the symmetrical plane, the nodes on the left-hand side boundary are allowed to translate in the y direction. The size of the domain was carefully chosen so that the developed velocity field are all well located within the domain. The trapdoor and the bottom boundaries extending both sides are assumed to be rigid, and the surface roughness of the trapdoor is fully rough since we assumed that the underlying soil is fully connected to the soil mass above the trapdoor.

An automatic mesh refinement technique was adopted to

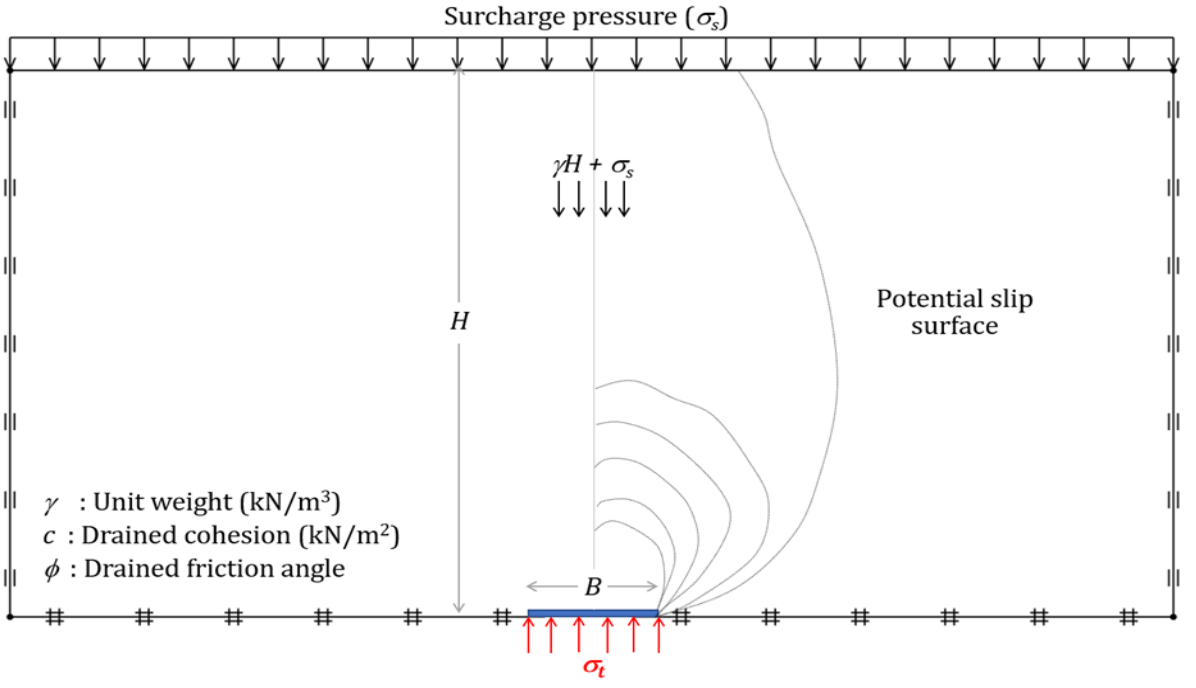

Fig. 1 Planar trapdoor - problem definition.

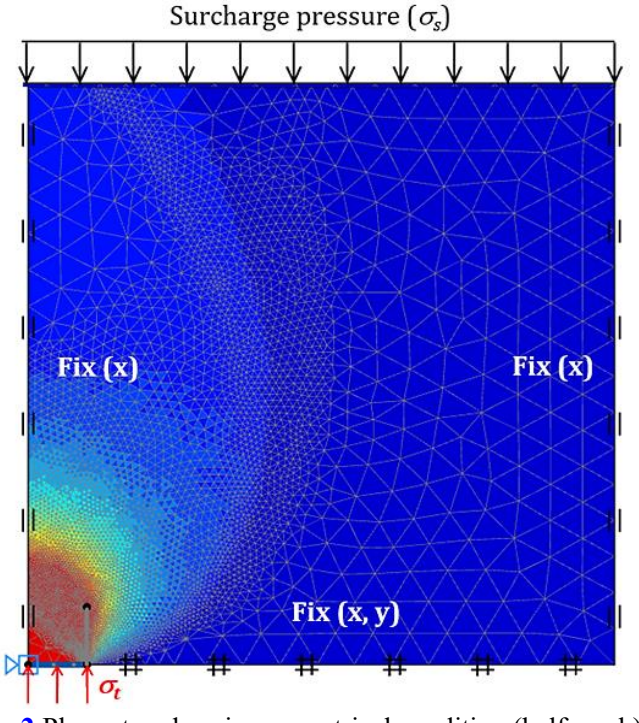

Fig. 2 Planar trapdoor in symmetrical condition (half mesh) - adaptive mesh, boundary condition, and shear dissipation.

construct UB and LB solutions of σ_t. The automated adaptive mesh refinement approach is one of OptumCE's sophisticated features. Utilizing the adaptive mesh techniques, meshes will automatically enlarge in sensitive zones with considerable plastic shearing strain. All numerical simulations employ 5,000 to 10,000 elements as the initial and goal number of elements, respectively with five adaptive iterations. This study used 5,000 to 10,000 elements since the accuracy of the results is based on the number of mesh elements and the phases technique. More elements may signify a more sensitive stress zone, which leads to a more exact answer, but not more than 10,000 elements since they have little influence on the solution, and it may take up unnecessary CPU time and computer memory.

To obtain the comprehensive stability coefficients (F_c, F_s, and F_γ), it is needed to determine the critical support pressure (σ_t) with the respective input parameters in equation (1). Note that the chosen range of soil friction angle ϕ is from 0° to 40° and the depth ratio H/D is from 0.5 to 10. This would cover most practical ranges in design practice. More details on how to obtain the individual coefficients are discussed below.

2.2 The cohesion coefficient

To determine the cohesion coefficient (F_c), it is needed to obtain a solution for σ_t, while providing two "artificial" zero parameters: namely $\sigma_s = 0$ and $\gamma = 0$. In this way, equation (1) is reduced to $\sigma_t = -cF_c$, where $F_c = -\sigma_t/c$.

A total of 902 FELAs were studied for F_c. For the wide range of parameters (ϕ = 0°to 40° and H/B = 0.5 to 10), the upper and lower bound results of σ_t were computed for F_c. The resulting F_c is shown in Fig. 3, where the figure shows that, as ϕ increases, the cohesion coefficient F_c decreases for all values of H/B. Note that a large cover-depth ratio of H/B leads to a large F_c value. Except for the line with H/B = 0.5 and 1.0, all curves of F_c are met at approximately ϕ = 31° and merge into one line afterward. Extremely tight bounds are achieved in this study, suggesting that the produced solutions are accurate.

2.3 The surcharge coefficient

In a similar way to the determination of F_c, the surcharge coefficient (F_s) can be obtained using both c = 0 and $\gamma = 0$ in the computations. Equation (1) reduces to $\sigma_t = \sigma_s F_s$ and the

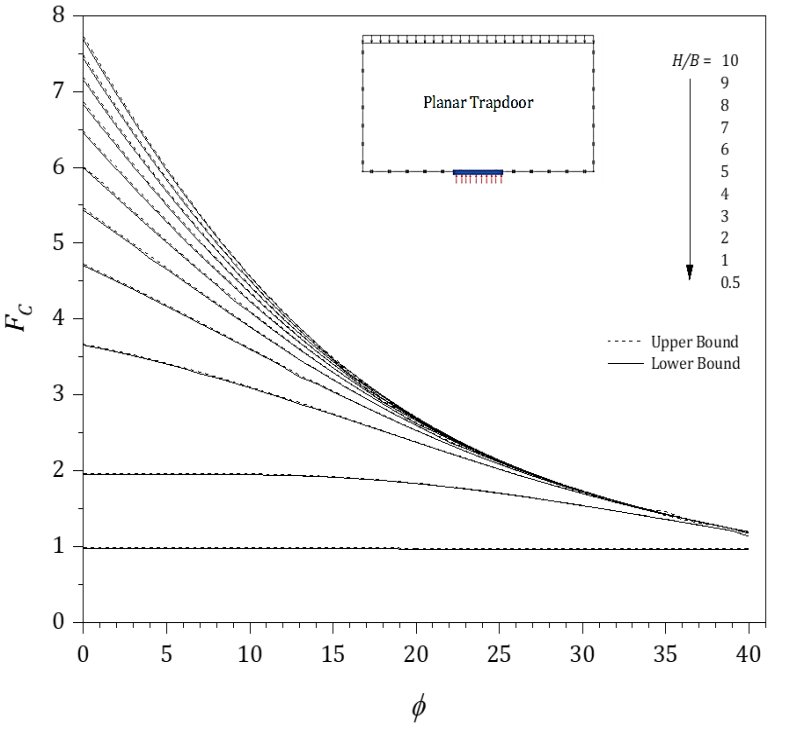

Fig. 3 Planar trapdoors - F_c vs ϕ (*LB* and *UB*) for various depth ratios (*H/B* = 0.5-10).

surcharge coefficient becomes $F_s = \sigma_t/\sigma_s$. For the wide range of parameters (ϕ = 0˚to 40˚ and *H/B* = 0.5 to10), a total of 902 FELAs was performed to obtain the upper and lower bound σ_t by using a constant surface pressure σ_s. The resulting surcharge coefficients are shown in Fig. 4.

Numerical results in Fig. 4 show that F_s = 1 for all *H/B* ratios of undrained clay (ϕ = 0˚). As ϕ increases, F_s decreases dramatically owing to the soil arching effect. It is interesting to see that F_s reduces to zero at ϕ = 40˚, except for the shallow case *H/B* = 0.5. Furthermore, numerical results have also shown that a larger *H/B* value leads to smaller F_s. In summary, less surcharge effect is expected for deeper trapdoors.

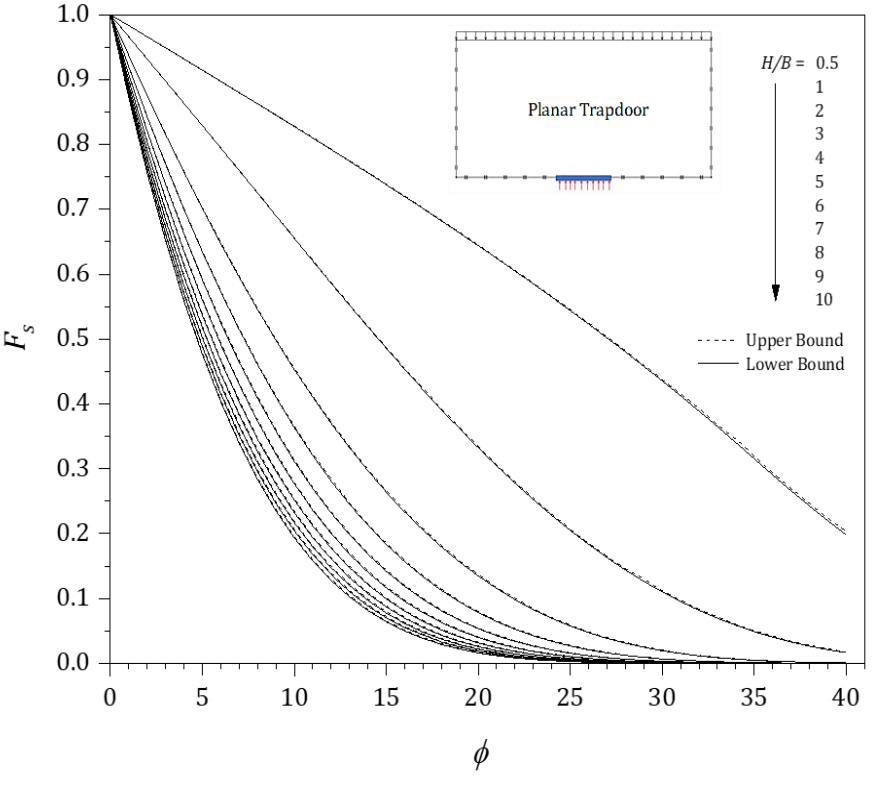

Fig. 4 Planar trapdoors - F_s vs ϕ (*LB* and *UB*) for various depth ratios (*H/B* = 0.5-10).

2.4 The unit weight coefficient

In order to study the soil unit weight coefficient (F_γ), it is necessary to put zero values of cohesion (c) and surcharge (σ_s) in all computations. Equation (1) then reduces to $\sigma_t = \gamma B F_\gamma$. Also, note that the parameter "D" in equation (1) is equivalent to "B" for a 2D planar trapdoor. A total of 902 *FELA* runs were studied for σ_t. The unit weight coefficients (F_γ) are then calculated using $F_\gamma = (\sigma_t/\gamma B)$, with given constant values of γ and B in all computations.

Figure 5 presents the effect of ϕ on F_γ for a wide range of H/B ratios. Numerical results have shown that F_γ is maximum at $\phi = 0^\circ$, and it decreases dramatically with the increasing ϕ for all curves. Interestingly, the maximum F_γ value for each depth ratio (H/B) coincides with the respective value of (H/B) for all curves presented. Note that all curves merge into one at $\phi = 40^\circ$ with an approximate minimum value of $F_\gamma = 0.03$. Also, the F_γ value for $H/B = 0.5$ seems to have a concave relationship with the increase in ϕ. For $H/B = 1$, F_γ decreases linearly with the increase in ϕ. For $H/B > 2$, a convex relationship between F_γ and ϕ is shown. The results in Fig. 5 also show that a smaller H/B leads to a lower value of F_γ. The unit weight effects become greater as the trapdoor depth increases.

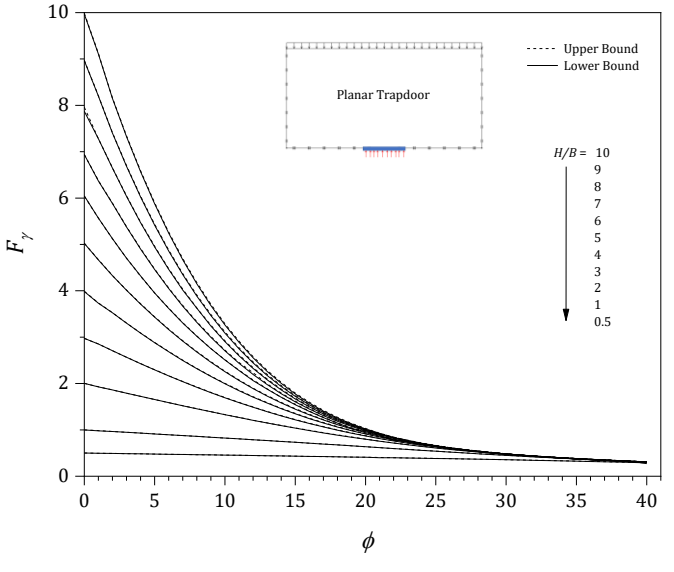

Fig. 5 Planar trapdoors - F_γ vs ϕ (*LB* and *UB*) for various depth ratios (H/B = 0.5-10).

Owing to the space limit, only the three lower bounds coefficients are presented in Tables A1-A3 in Appendix for the 2D planar trapdoors.

2.5 Comparison with published results

Although there are very few published results that can be used to compare with our stability coefficients, the produced upper and lower limits do offer an in-built comparison and therefore would increase user confidence. Nevertheless, comparing the bound solutions with other accessible options would further improve the credibility and feasibility in practice, in spite that it is not mandatorily necessary due to the tight bounds produced in the current study. Since only F_c is available in the literature, a comparison of F_c with those published results is made in Fig. 6. The comparison is for a planar trapdoor in undrained conditions with $\phi = 0^\circ$. Numerical results have shown that the analytical bounding solutions in Davis[63] and Gunn[64] have been considerably improved, whereas the linear programming approach by Sloan *et al.*[15] agrees with the current results by around 10%. Also, the recently reported solutions by Shiau and Hassan[65] are remarkably close to those in the current investigation. To our best knowledge, there are no published solutions of F_s and F_γ that we can use to compare the current results with.

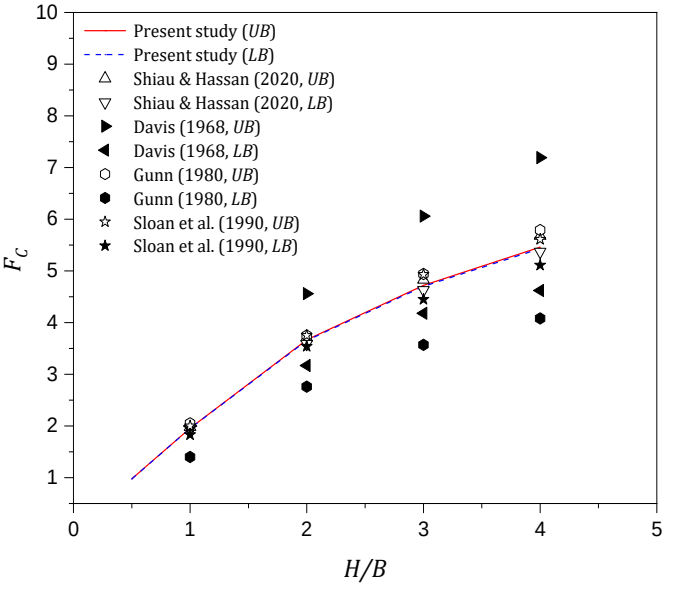

Fig. 6 Comparison of F_c with published literature (planar trapdoors, undrained, $\phi = 0^\circ$).

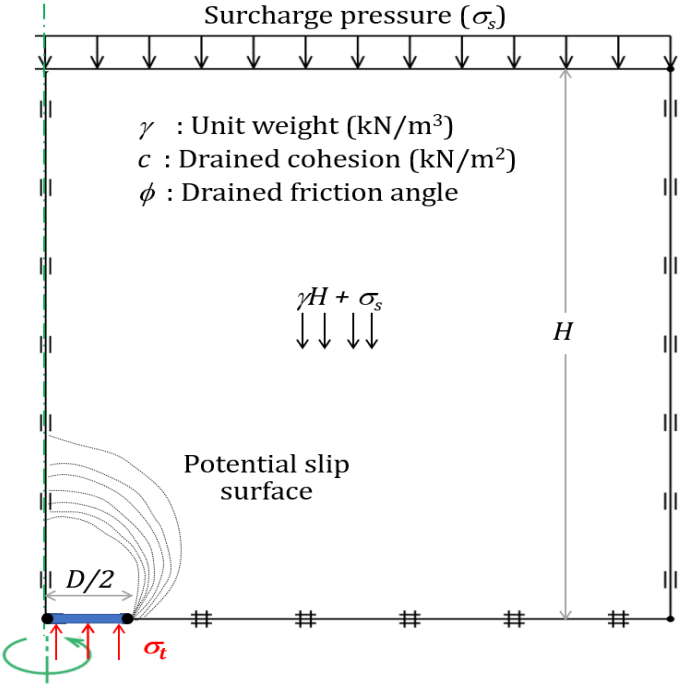

Fig. 7 3D circular trapdoor in 2D axisymmetric condition - problem definition.

3. 3D Circular Trapdoor in Axisymmetry

3.1 Problem statement and FELA modeling

The problem description of a circular trapdoor in axial symmetry is shown in Fig. 7. The circular trapdoor is covered with a depth (H) and has a diameter (D). The ground surface has a vertical surcharge (σ_s), and the normal pressure on the trapdoor is represented by (σ_t). The circular trapdoor is in axial symmetry, representing a true 3D circular trapdoor.

Figure 8 presents a typical axisymmetric mesh with a shear dissipation plot of the FELA analysis. Same as in the planar trapdoor, the soil mass consists of several triangular elements and is simulated using the Mohr-Coulomb material. The bottom boundary is fixed in both x- and y-directions (except for the trapdoor length), while the left and the right boundary allows movement in the y-direction only. The size of the model domain is selected to be large enough so that the overall velocity field would not interfere with the boundary conditions. Other details are similar to those in Section 2.1. Using both the UB and LB simulations, a complete set of stability coefficients (F_c, F_s, and F_γ) is developed that can be used to evaluate critical support pressures (σ_t) in drained conditions. The following sections discuss the details involved in determining individual coefficients.

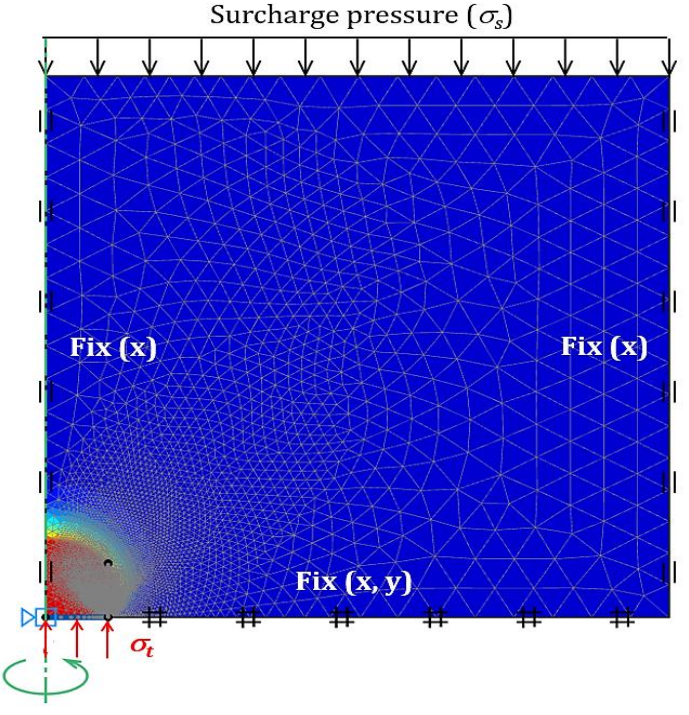

Fig. 8 3D circular trapdoor in 2D axisymmetric condition - adaptive mesh, boundary condition, and shear dissipation.

3.2 The cohesion coefficient

Using two "artificial" zero parameters, namely $\sigma_s = 0$ and $\gamma = 0$, a total of 902 FELA simulations were carried out to compute the upper and lower bounds of σ_t for the wide range of parameters ($\phi = 0^\circ$ to 40° and $H/D = 0.5$ to 10). The cohesion coefficients (F_c) were then computed using $\sigma_t = -cF_c$. The complete set of F_c results is presented in Fig. 9.

Numerical results in Fig. 9 have shown that as the internal soil friction angle ϕ increases, the cohesion coefficient F_c decreases. This occurs for all values of H/D ratios. A larger H/D ratio leads to a higher F_c value. All curves combine into a single one at $\phi = 27^\circ$, except for the line with $H/D = 0.5$. This is mainly due to the stability response of a shallow case, where soil arching is comparatively less than the other H/D ratios. It is not surprising to see that the axisymmetric results of F_c are consistently greater than those from the planar trapdoor in Fig. 3 by 1.5 to 2 times. A less conservative design can always be achieved by using the current axisymmetric coefficients.

3.3 The surcharge coefficient

Just like in the planar trapdoor, the surcharge stability coefficient (F_s) is computed using both ($c = 0$) and ($\gamma = 0$), and equation (1) consequently reduces to $\sigma_t = \sigma_s F_s$. With a constant value of σ_s, 902 FELAs were performed in this study. The obtained σ_t were then used to calculate surcharge stability coefficients ($F_s = \sigma_t/\sigma_s$).

Figure 10 shows the complete results of surcharge stability coefficients (F_s). Numerical results have shown that the surcharge stability coefficient F_s decreases from unity (where $\phi = 0^\circ$) with an increase in ϕ. A higher H/D value results in a lower value of F_s. Numerical results have also shown that F_s decreases to zero at different values of ϕ and H/D. The deeper the H/D, the smaller the ϕ for zero value of F_s. It is generally understood that the greater the ϕ, the larger the soil arching effects. Also, the deeper the trapdoor, the less the surcharge effects. In comparison with the planar trapdoor in Fig. 4, the axisymmetric (AX) results produce smaller values of F_s and therefore they are less conservative than those in the planar trapdoor.

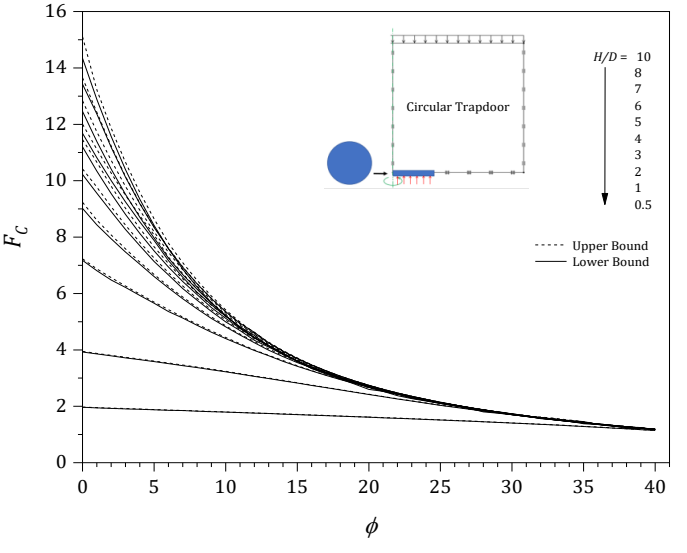

Fig. 9 3D Circular trapdoors in axisymmetric condition - F_c vs ϕ (*LB* and *UB*) for various depth ratios (H/D = 0.5-10).

3.4 The unit weight coefficient

To determine the unit weight coefficient (F_γ), equation (1) is simplified to $\sigma_t = \gamma D F_\gamma$ by using two "artificial" zero parameters: namely $c = 0$ and $\sigma_s = 0$. A total of 902 FELAs

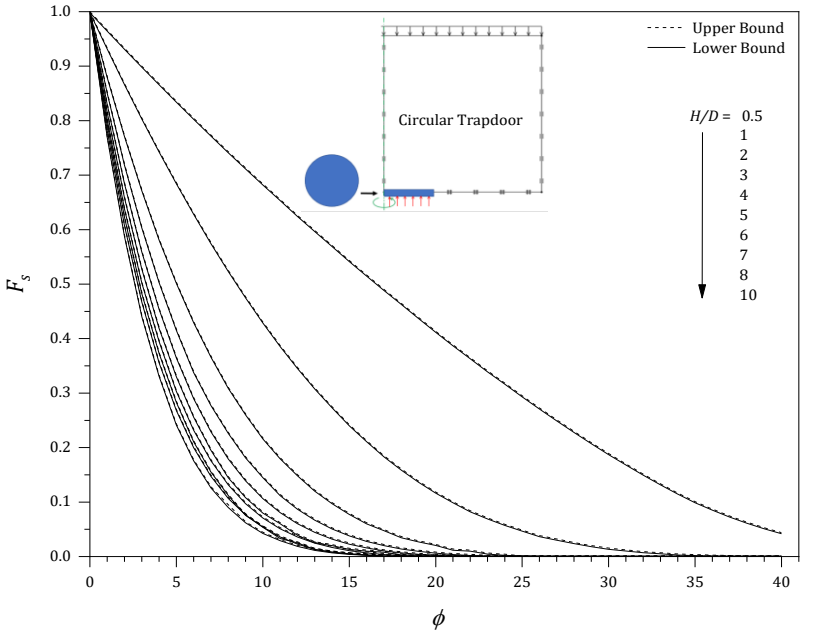

Fig. 10 3D Circular trapdoors in axisymmetric condition - F_s vs ϕ (*LB* and *UB*) for various depth ratios (H/D = 0.5-10).

were computed for σ_t with constant values of γ and D. The unit weight coefficients (F_γ) can be calculated using $F_\gamma = (\sigma_t/\gamma D)$. The complete results of F_γ are presented in Fig. 11. Numerical results in Fig. 11 have shown that F_γ is maximum at $\phi = 0^\circ$ and it decreases as ϕ increases. Interestingly, the F_γ at $\phi = 0^\circ$ (undrained condition) for 3D circular trapdoors are equal to those 2D planar ones in Fig. 5, i.e., $F_\gamma = H/D$ at $\phi = 0^\circ$. The larger the ϕ value, the smaller the F_γ. All curves combine into one at approximately $\phi > 30^\circ$, and a minimum value of $F_\gamma = 0.016$ is obtained at $\phi = 40^\circ$, indicating the minimum supporting pressure for "dry" sand.

Owing to the space limit, only the three lower bounds coefficients are presented in Tables A4-A6 in Appendix for the 3D circular trapdoors.

3.5 Comparison with published results

For the undrained circular trapdoor, Shiau *et al.*[5] reported rigorous three-dimensional solutions of UB and LB using FELA, whilst Keawsawasvong and Shiau[18] presented non-homogenous solutions using two-dimensional axisymmetric FELA with UB and LB. The two published undrained results are used for comparison purposes in this section. There are currently no other drained results of F_s and F_γ that can be used to compare with.

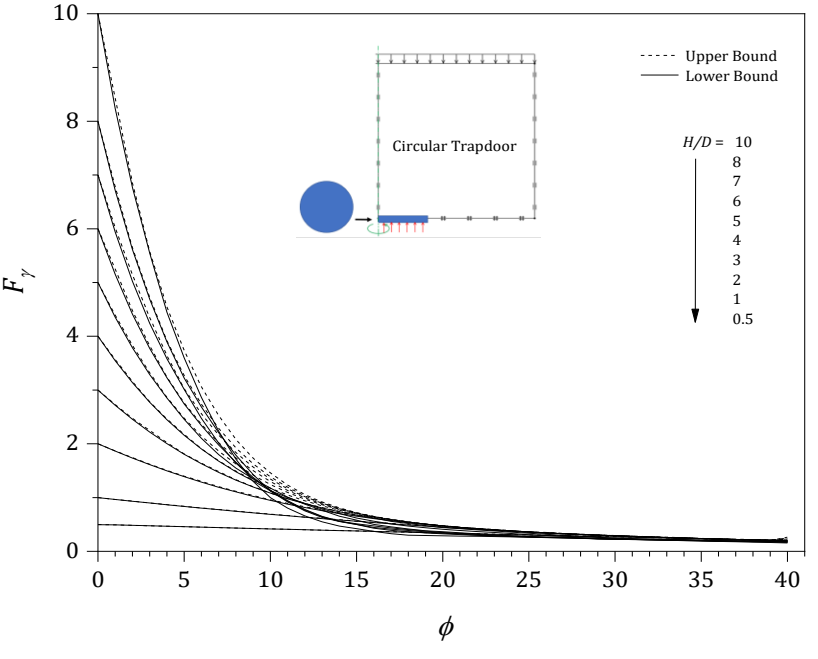

Fig. 11 3D Circular trapdoors in axisymmetric condition - F_γ vs ϕ (*LB* and *UB*) for various depth ratios (H/D = 0.5-10).

Figure 12 presents a comparison of F_c values for 3D circular trapdoors under undrained conditions with $\phi = 0^\circ$. Overall, it is pleased to see that the results are in excellent agreement. Although there are no existing F_s and F_γ results to compare with, the credibility and practicability of this study have greatly been improved with the current comparison as well as the produced tight bounds (UB and LB) in the present study.

4. Examples and comparisons of 2D and 3D

Example 1: An underground cavity in greenfield condition ($\sigma_s = 0$) has a width B (or a diameter D) of 2 m. The cover depth (H) is 2 m. The soil is assumed to have cohesion ($c = 17$ kPa). The soil unit weight is 16 kN/m^3, and the internal friction angle of the soil ϕ is 10˚. Determine the required support pressure σ_t to maintain the sinkhole stability using the produced coefficients in the 2D planar trapdoor and 3D circular trapdoors.

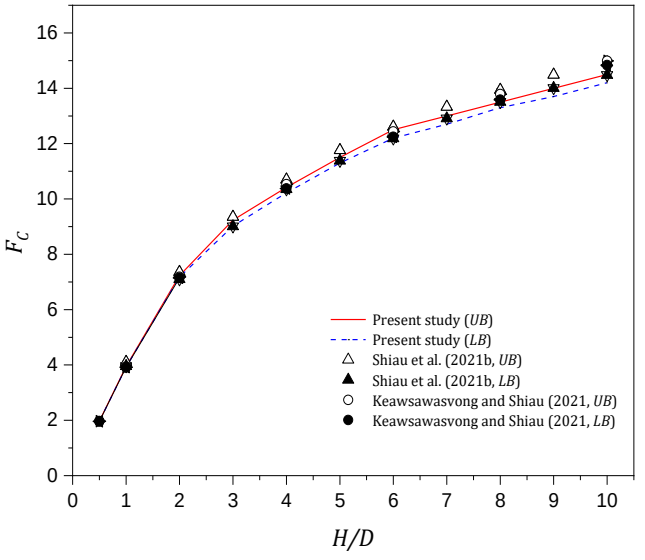

Fig. 12 Comparison of F_c with published literature (3D circular trapdoors, undrained, $\phi = 0^\circ$)

2D planar trapdoor

For $H/B = 1$ and $\phi = 10^\circ$, Tables A1, A2 and A3 provide values of lower bound $F_c = 1.951$, $F_s = 0.655$, and $F_\gamma = 0.824$. Since no surcharge loading ($\sigma_s = 0$), equation (1) reduces to $\sigma_t = -cF_c + \gamma BF_\gamma$. Substituting c, γ, B, F_c, and F_γ into the equation, σ_t is computed as –6.80 kPa. Note that the negative value σ_t represents that a tensile pressure is needed to bring the system to fail. In other words, the trapdoor is theoretically stable on its own when $\sigma_t = 0$ (without the pulling pressure). The actual computer analysis using the parameters gives a value of –6.82 kPa.

3D circular trapdoor

For $H/D = 1$ and $\phi = 10^\circ$, Tables A4, A5, and A6 provide values of lower bounds $F_c = 3.223$, $F_s = 0.429$, and $F_\gamma = 0.688$. Substituting c, γ, B, F_c, and F_γ into the equation $\sigma_t = -cF_c + \gamma DF_\gamma$, σ_t is computed as a negative value of -32.78 kPa. Same as in the 2D planar trapdoor, the trapdoor is stable on its own when $\sigma_t = 0$ (without the pulling pressure). Compared to the 2D planar trapdoor ($\sigma_t = -6.80$ kPa), a less conservative design can be achieved by using the 3D circular trapdoor result ($\sigma_t = -32.78$ kPa). For comparison, the actual computer analysis gives a value of –33.2 kPa, which has provided a good level of confidence in using the table solution.

Example 2: Same as in Example 1, except that now $\sigma_s = 100$ kPa, determine the minimum pressure σ_t to maintain the sinkhole stability using the produced stability coefficients in the 2D planar trapdoor and 3D circular trapdoors.

2D planar trapdoor

For $H/B = 1$ and $\phi = 10^\circ$, Tables A1, A2, and A3 provide values of lower bounds $F_c = 1.951$, $F_s = 0.655$, and $F_\gamma = 0.824$. Substituting all the parameters into equation (1), σ_t is 58.70 kPa. The positive value of σ_t simply means that a support pressure is needed so that the trapdoor would not fail. In other words, the trapdoor is unstable on its own without the support pressure (i.e. when $\sigma_t = 0$). The actual computer analysis using the parameters gives a value of 58.68 kPa.

3D circular trapdoor

For $H/B = 1$ and $\phi = 10^\circ$, Tables A4, A5 and A6 provide values of lower bounds $F_c = 3.223$, $F_s = 0.429$, and $F_\gamma = 0.688$. Substituting all the parameters into equation (1), σ_t is calculated as 10.13 kPa. Again, the positive value of σ_t represents a need for support pressure in order to prevent trapdoor failure. Compared to the 2D planar trapdoor ($\sigma_t = 58.70$ kPa), much less support pressure ($\sigma_t = 10.13$ kPa) is predicted using the 3D circular trapdoor analysis. Therefore, it can be concluded that less conservative design can always be achieved by using sophisticated 3D analysis. For comparison purposes, the actual computer analysis gives a value of 9.74 kPa, indicating that the solution is both efficient and effective, and can be used by practical engineers with great confidence.

5. Conclusions

Using the superposition method of Terzaghi's bearing capacity coefficients, this paper has successfully produced three rigorous stability coefficients (F_c, F_s, and F_γ) that can be used to determine the drained stability of 2D planar trapdoors and 3D circular trapdoors in axisymmetry. The current study contributes in several ways to our understanding of using stability coefficients to determine limit loads. The following conclusions are drawn based on the current study.

1. The three stability coefficients (F_c, F_s, and F_γ) are functions of soil internal friction angle (ϕ) and cover-depth ratio (H/B or

H/D). The critical support pressure ($\sigma_t = -cF_c + \sigma_s F_s + \gamma D F_\gamma$) can be conveniently determined in a similar way as in Terzaghi's classic bearing capacity problem using the principle of superposition. It can be used in either drained or undrained conditions, as well as to study the effect of surcharge.

2. The illustrated example has proven that the stability coefficient approach is both convenient and accurate in the calculation of critical pressures. Numerical results have shown that the axisymmetric 3D circular trapdoor results would yield a less conservative design, in comparison with the conservative 2D planar trapdoor idealization.

3. The current solutions are limited to the cases of planar and circular trapdoors in homogeneous soils, which cannot be used in the cases of rectangular trapdoors and trapdoors in layered soils. It is recommended that future work direction can be pointed to non-homogenous effects on the three stability coefficients. The classical passive trapdoor problems can also be investigated using the proposed three stability coefficients.

Acknowledgment

This work was supported by the Thailand Science Research and Innovation Fundamental Fund fiscal year 2023. The fourth author (V. Kamchoom) acknowledges the grant (FRB66065/0258-RE-KRIS/FF66/53) from King Mongkut's Institute of Technology Ladkrabang (KMITL) and National Science, Research and Innovation Fund (NSRF), the grant (N10A650844) under Climate Change and Climate Variability Research in Monsoon Asia (CMON3) from the National Research Council of Thailand (NRCT) and the National Natural Science Foundation of China (NSFC).

Conflict of Interest

There is no conflict of interest.

Supporting Information

Applicable.

References

[1] G. Enstad, On the theory of arching in mass flow hoppers, *Chemical Engineering Science*, 1975, **30**, 1273-1283, doi: 10.1016/0009-2509(75)85051-2.

[2] M. Fraldi, F. Guarracino, Limit analysis of collapse mechanisms in cavities and tunnels according to the Hoek-Brown failure criterion, *International Journal of Rock Mechanics and Mining Sciences*, 2009, **46**, 665-673, doi: 10.1016/j.ijrmms.2008.09.014.

[3] A. M. Suchowerska, R. S. Merifield, J. P. Carter, J. Clausen, Prediction of underground cavity roof collapse using the Hoek-Brown failure criterion, *Computers and Geotechnics*, 2012, **44**, 93-103, doi: 10.1016/j.compgeo.2012.03.014.

[4] J. Shiau, B. Chudal, K. Mahalingasivam, S. Keawsawasvong, Pipeline burst-related ground stability in blowout condition, *Transportation Geotechnics*, 2021, **29**, 100587, doi: 10.1016/j.trgeo.2021.100587.

[5] J. Shiau, J. S. Lee, F. Al-Asadi, Three-dimensional stability analysis of active and passive trapdoors, *Tunnelling and Underground Space Technology*, 2021, **107**, 103635, doi: 10.1016/j.tust.2020.103635.

[6] J. Shiau, S. Keawsawasvong, B. Chudal, K. Mahalingasivam, S. Seehavong, Sinkhole stability in elliptical cavity under collapse and blowout conditions, *Geosciences*, 2021, **11**, 421, doi: 10.3390/geosciences11100421.

[7] J. Shiau, S. Keawsawasvong, J.-S. Lee, Three-dimensional stability investigation of trapdoors in collapse and blowout conditions, *International Journal of Geomechanics*, 2022, **22**, doi: 10.1061/(asce)gm.1943-5622.0002339.

[8] J. Shiau, B. Chudal, S. Keawsawasvong, Three-dimensional sinkhole stability of spherical cavity, *Acta Geotechnica*, 2022, **17**, 3947-3958, doi: 10.1007/s11440-022-01522-8.

[9] G. R. Iglesia, H. H. Einstein, R. V. Whitman, Validation of centrifuge model scaling for soil systems via trapdoor tests, *Journal of Geotechnical and Geoenvironmental Engineering*, 2011, **137**, 1075-1089, doi: 10.1061/(asce)gt.1943-5606.0000517.

[10] G. R. Iglesia, H. H. Einstein, R. V. Whitman, Investigation of soil arching with centrifuge tests, *Journal of Geotechnical and Geoenvironmental Engineering*, 2014, **140**, 04013005, doi: 10.1061/(asce)gt.1943-5606.0000998.

[11] B. Chevalier, G. Combe, P. Villard, Experimental and discrete element modeling studies of the trapdoor problem: influence of the macro-mechanical frictional parameters, *Acta Geotechnica*, 2012, **7**, 15-39, doi: 10.1007/s11440-011-0152-5.

[12] T. Tadatsugu, Progressive failure and scale effect of trap-door problems with granular materials, *Soils and Foundations*, 1993, **33**, 11-22, doi: 10.3208/sandf1972.33.11.

[13] N. C. Koutsabeloulis, D. V. Griffiths, Numerical modelling of the trap door problem, *Géotechnique*, 1989, **39**, 77-89, doi: 10.1680/geot.1989.39.1.77.

[14] C. M. Martin, Undrained collapse of a shallow plane-strain trapdoor, Géotechnique, 2009, **59**, 855-863, doi: 10.1680/geot.8.t.023.

[15] S. W. Sloan, A. Assadi, N. Purushothaman, Undrained stability of a trapdoor, Géotechnique, 1990, **40**, 45-62, doi: 10.1680/geot.1990.40.1.45.

[16] Boonchai, Ukritchon, Three-dimensional stability analysis of the collapse pressure on flexible pavements over rectangular trapdoors, *Transportation Geotechnics*, 2019, **21**, 100277, doi: 10.1016/j.trgeo.2019.100277.

[17] S. Keawsawasvong, S. Likitlersuang, Undrained stability of active trapdoors in two-layered clays, *Underground Space*, 2021, **6**, 446-454, doi: 10.1016/j.undsp.2020.07.002.

[18] S. Keawsawasvong, J. Shiau, Stability of active trapdoors in axisymmetry, *Underground Space*, 2022, **7**, 50-57, doi: 10.1016/j.undsp.2021.05.001.

[19] H. Rai, S. Keawsawasvong, J. T. Chavda, Numerical investigations on evaluation of undrained stability of active and passive strip, circular, and annular trapdoors, *Geotechnical and Geological Engineering*, 2023, **41**, 673-684, doi: 10.1007/s10706-022-02294-4.

[20] J. Shiau, S. Keawsawasvong, S. Seehavong, Stability of unlined elliptical tunnels in rock masses, *Rock Mechanics and Rock Engineering*, 2022, **55**, 7307-7330, doi: 10.1007/s00603-022-02996-4.
[21] J. Shiau, S. Keawsawasvong, Producing undrained stability factors for various tunnel shapes, *International Journal of Geomechanics*, 2022, **22**, 06022017, doi: 10.1061/(asce)gm.1943-5622.0002487.
[22] J. Shiau, K. Mahalingasivam, B. Chudal, S. Keawsawasvong, Pipeline burst-related soil stability in collapse condition, *Journal of Pipeline Systems Engineering and Practice*, 2022, **13**, 04022019, doi: 10.1061/(asce)ps.1949-1204.0000657.[LinkOut]
[23] J. Shiau, S. Keawsawasvong, J.-S. Lee, M. M. Hassan, Three-dimensional circular trapdoor stability, *Transportation Infrastructure Geotechnology*, 2022, **9**, 173-184, doi: 10.1007/s40515-021-00166-7.
[24] F. Lai, J. Shiau, S. Keawsawasvong, F. Chen, R. Banyong, S. Seehavong, Physics-based and data-driven modeling for stability evaluation of buried structures in natural clays, *Journal of Rock Mechanics and Geotechnical Engineering*, 2022, doi: 10.1016/j.jrmge.2022.07.006.
[25] S. Keawsawasvong, Limit analysis solutions for spherical cavities in sandy soils under overloading, *Innovative Infrastructure Solutions*, 2020, **6**, 1-8, doi: 10.1007/s41062-020-00398-5.
[26] S. Keawsawasvong, B. Ukritchon, Undrained stability of a spherical cavity in cohesive soils using finite element limit analysis, *Journal of Rock Mechanics and Geotechnical Engineering*, 2019, **11**, 1274-1285, doi: 10.1016/j.jrmge.2019.07.001.
[27] J. Shiau, F. Al-Asadi, Three-dimensional heading stability of twin circular tunnels, *Geotechnical and Geological Engineering*, 2020, **38**, 2973-2988, doi: 10.1007/s10706-020-01201-z.
[28] J. Shiau, F. Al-Asadi, Twin tunnels stability factors F_c, F_s and F_γ, *Geotechnical and Geological Engineering*, 2021, **39**, 335-345, doi: 10.1007/s10706-020-01495-z.
[29] J. Shiau, S. Keawsawasvong, W. Yodsomjai, Determination of support pressure for the design of square box culverts, International Journal of Geomechanics, 2023, **23**, 06022035, doi: 10.1061/(asce)gm.1943-5622.0002620.
[30] G, Anagnostou, Face stability conditions with earth-pressure-balanced shields, *Tunnelling and Underground Space Technology*, 1996, **11**, 165-173, doi: 10.1016/0886-7798(96)00017-X.
[31] S. W. Sloan, Geotechnical stability analysis, Géotechnique, 2013, **63**, 531-571, doi: 10.1680/geot.12.rl.001.
[32] OptumCE 2020, OptumG2. Copenhagen, Denmark: *Optum Computational Engineering*. Available no: https://optumce.com/.
[33] Q. T. Huynh, V. Q. Lai, J. Shiau, S. Keawsawasvong, L. Z. Mase, H. T. Tra, On the use of both diaphragm and secant pile walls for a basement upgrade project in Vietnam, *Innovative Infrastructure Solutions*, 2021, **7**, 1-10, doi: 10.1007/s41062-021-00625-7.
[34] Q. T. Huynh, H. T. Tra, L. Z. Mase, N. H. Vo, V. Q. Lai, Analysing allowable horizontal displacements of retaining wall based on limited settlements of Adjacent Building. *Geotechnical Engineering*, 2022, **53**, 1-10.
[35] L. Z. Mase, Refrizon, Rosiana, P. W. Anggraini, Local site investigation and ground response analysis on downstream area of muara bangkahulu river, bengkulu city, Indonesia, *Indian Geotechnical Journal*, 2021, **51**, 952-966, doi: 10.1007/s40098-020-00480-w.
[36] L. Z. Mase, V. Febriyanto, Numerical analysis of jetty platform countermeasure effort at muaro kualo area in bengkulu city, Indonesia, *Transportation Infrastructure Geotechnology*, 2022, 1-25, doi: 10.1007/s40515-022-00258-y.
[37] L. Z. Mase, K. Amri, M. Farid, F. Rahmat, M. Nur Fikri, J. Saputra, S. Likitlersuang, Effect of water level fluctuation on riverbank stability at the estuary area of muaro kualo segment, muara bangkahulu river in bengkulu, Indonesia, *Engineering Journal*, 2022, **26**, 1-16, doi: 10.4186/ej.2022.26.3.1.
[38] L. Z. Mase, A. F. Edriani, H. Putra, Hardiansyah, J. Saputra, Bearing capacity analysis of surficial strip footing at sub-watershed of downstream Muara Bangkahulu River, Indonesia, *IOP Conference Series: Earth and Environmental Science*, 2021, **871**, 012051, doi: 10.1088/1755-1315/871/1/012051.
[39] L. Z. Mase, A. Perdana, Hardiansyah, K. Amri, S. Bahri, A case study of slope stability improvement in central bengkulu landslide in Indonesia, *Transportation Infrastructure Geotechnology*, 2022, **9**, 442-466, doi: 10.1007/s40515-021-00186-3.
[40] B. Ukritchon, J. C. Faustino, S. Keawsawasvong, Numerical investigations of pile load distribution in pile group foundation subjected to vertical load and large moment, *Geomechanics and Engineering*, 2016, **10**, 577-598, doi: 10.12989/gae.2016.10.5.577.
[41] S. Likitlersuang, P. Pholkainuwatra, T. Chompoorat, S. Keawsawasvong, Numerical modelling of railway embankments for high-speed train constructed on soft soil, *Journal of GeoEngineering*, 2018, **13**, 149-159, 10.6310/jog.201809_13(3).6
[42] S. Keawsawasvong, B. Ukritchon, Failure modes of laterally loaded piles under combined horizontal load and moment considering overburden stress factors, *Geotechnical and Geological Engineering*, 2020, **38**, 4253-4267, doi: 10.1007/s10706-020-01293-7.
[43] S. W. Sloan, Lower bound limit analysis using finite elements and linear programming, *International Journal for Numerical and Analytical Methods in Geomechanics*, 1988, **12**, 61-77, doi: 10.1002/nag.1610120105.
[44] S. W. Sloan, Upper bound limit analysis using finite elements and linear programming, *International Journal for Numerical and Analytical Methods in Geomechanics*, 1989, **13**, 263-282, doi: 10.1002/nag.1610130304.
[45] A. V. Lyamin, S. W. Sloan, Lower bound limit analysis using non-linear programming, *International Journal for Numerical Methods in Engineering*, 2002, **55**, 573-611, doi: 10.1002/nme.511.
[46] A. V. Lyamin, S. W. Sloan, Upper bound limit analysis using linear finite elements and non-linear programming, *International*

Journal for Numerical and Analytical Methods in Geomechanics, 2002, **26**, 181-216, doi: 10.1002/nag.198.
[47] K. Krabbenhøft, A. V. Lyamin, S. W. Sloan, Formulation and solution of some plasticity problems as conic programs, *International Journal of Solids and Structures*, 2007, **44**, 1533-1549, doi: 10.1016/j.ijsolstr.2006.06.036.
[48] W. Yodsomjai, S. Keawsawasvong, V. Q. Lai, Limit analysis solutions for bearing capacity of ring foundations on rocks using hoek-brown failure criterion, *International Journal of Geosynthetics and Ground Engineering*, 2021, **7**, 1-10, doi: 10.1007/s40891-021-00281-y.
[50] W. Yodsomjai, S. Keawsawasvong, S. Likitlersuang, Stability of unsupported conical slopes in hoek-brown rock masses, *Transportation Infrastructure Geotechnology*, 2021, **8**, 279-295, doi: 10.1007/s40515-020-00137-4.
[51] S. Keawsawasvong, C. Thongchom, S. Likitlersuang, Bearing capacity of strip footing on hoek-brown rock mass subjected to eccentric and inclined loading, *Transportation Infrastructure Geotechnology*, 2021, **8**, 189-202, doi: 10.1007/s40515-020-00133-8.
[52] S. Keawsawasvong, B. Ukritchon, Undrained basal stability of braced circular excavations in non-homogeneous clays with linear increase of strength with depth, *Computers and Geotechnics*, 2019, **115**, 103180, doi: 10.1016/j.compgeo.2019.103180.
[53] S. Keawsawasvong, K. Yoonirundorn, T. Senjuntichai, Pullout capacity factor for cylindrical suction caissons in anisotropic clays based on anisotropic undrained shear failure criterion, *Transportation Infrastructure Geotechnology*, 2021, **8**, 629-644, doi: 10.1007/s40515-021-00154-x.
[54] S. Keawsawasvong, J. Shiau, C. Ngamkhanong, V. Qui Lai, C. Thongchom, Undrained stability of ring foundations: axisymmetry, anisotropy, and nonhomogeneity, *International Journal of Geomechanics*, 2022, **22**, 04021253, doi: 10.1061/(asce)gm.1943-5622.0002229.
[55] D. K. Nguyen, T. P. Nguyen, S. Keawsawasvong, V. Q. Lai, Vertical uplift capacity of circular anchors in clay by considering anisotropy and non-homogeneity, *Transportation Infrastructure Geotechnology*, 2022, **9**, 653-672, doi: 10.1007/s40515-021-00191-6.
[56] S. Keawsawasvong, Bearing capacity of conical footings on clays considering combined effects of anisotropy and non-homogeneity, *Ships and Offshore Structures*, 2022, **17**, 2317-2328, doi: 10.1080/17445302.2021.1987110.
[57] W. Yodsomjai, S. Keawsawasvong, C. Thongchom, J. Lawongkerd, Undrained stability of unsupported conical slopes in two-layered clays, *Innovative Infrastructure Solutions*, 2020, **6**, 1-17, doi: 10.1007/s41062-020-00384-x.
[58] S. Keawsawasvong, S. Seehavong, C. Ngamkhanong, Application of artificial neural networks for predicting the stability of rectangular tunnels in hoek-brown rock masses, *Frontiers in Built Environment*, 2022, **8**, 837745, doi: 10.3389/fbuil.2022.837745.
[59] V. B. Chauhan, P. Kumar, S. Keawsawasvong, Limit analysis solution for ultimate bearing capacity of footing resting on the rock mass with a circular void subjected to line loading, *Indian Geotechnical Journal*, 2022, 1-14, doi: 10.1007/s40098-022-00676-2.
[60] P. Kumar, V. B. Chauhan, Ultimate bearing capacity of a foundation on the rock media due to the presence of a circular void: design tables, failure mechanism, and recommendations, *Arabian Journal of Geosciences*, 2022, **15**, 1-11, doi: 10.1007/s12517-022-10620-6.
[61] P. Kumar, V. B. Chauhan, Bearing capacity of strip footing resting above a circular void in the rock mass using adaptive finite element method, *Innovative Infrastructure Solutions*, 2021, **7**, 1-14, doi: 10.1007/s41062-021-00666-y.
[62] P. Kumar, V. B. Chauhan, On the eccentrically loaded strip footing resting over a circular cavity in the rock mass: adaptive finite-element analysis, observations, and recommendations, *International Journal of Geomechanics*, 2023, **23**, 04022287, doi: 10.1061/ijgnai.gmeng-7985.
[63] E. H. Davis, Theories of plasticity and the failure of soil masses, In I. K. Lee (Ed.), Soil Mechanics: Selected Topics (pp. 341–380). London: Butterworths, 1968.
[64] M. J. Gunn, Limit analysis of undrained stability problems using a very small computer, In Proceedings of the Symposium on Computer Applications in Geotechnical Problems in Highway Engineering, Cambridge, 1980.
[65] J. Shiau, M. M. Hassan, Undrained stability of active and passive trapdoors, *Geotechnical Research*, 2020, **7**, 40-48, doi: 10.1680/jgere.19.00033.

Author Information

Dr. Suraparb Keawsawasvong *is a lecturer in the Department of Civil Engineering, Thammasat School of Engineering, Thammasat University, Thailand. He earned his bachelor's degree (Honors with highest GPA) from Thammasat University (2013). His master's and Ph.D. degrees were both from Chulalongkorn University (2015 and 2019, respectively). During his Ph.D. study, he was a visiting research student at the Faculty of Applied Sciences, Simon Fraser University, Canada. He was a geotechnical engineer at Strategia Engineering Consultants Co., Ltd. and Altemtech Co., Ltd. in the period 2015–2016. Dr. Suraparb's main research is in the areas of geomechanics, solid mechanics, finite element limit analysis, finite element method, deep excavations, optimizations, geotechnical stability analysis, and machine learning models for civil engineering problems.*